Acta Crystallographica Section B
Structural Science
ISSN 0108-7681

Model for the crystal packing and conformational changes of biphenyl in incommensurate phase transitions

Alexander Dzyabchenko[a,b] and Harold A. Scheraga[a]*

[a]Department of Chemistry and Biochemistry, Cornell University, Ithaca, NY 14853-1301, USA, and [b]Karpov Institute of Physical Chemistry, 10 Vorontsovo pole, 105064 Moscow, Russia

Correspondence e-mail: has5@cornell.edu

Received 21 January 2004
Accepted 9 February 2004

Standard atom–atom potentials for hydrocarbons and a torsional potential to account for the π-electron conjugation energy were used to model the crystal structures and phase transitions of biphenyl. The model describes the high-temperature phase (I) with its planar molecule as a stationary point of the energy hypersurface. Phase I represents a low-energy barrier between the symmetry minima of the ground state (phase III), in which the molecule is twisted with torsion angles of opposite sign. Global-energy minimization was carried out by considering both regular structures, with one or two independent molecules, and quasi-one-dimensional superstructures built of N cells (N up to 16) of the high-temperature structure. The various energy-minimized biphenyl structures demonstrate remarkable similarity in their crystal packing; in particular, there are characteristic rows of cooperatively twisted molecules parallel to the superstructure dimension b. The structures built of centrosymmetric rows ($P\bar{1}$, $Z = 4$ and 8) are almost as low in energy as the basic structure (an $N = 2$ superstructure, Pa, $Z = 4$); moreover, one of them is isostructural with the low-temperature p-quaterphenyl structure. With $N > 8$, structures of lower energy than that of the basic structure ($N = 2$) were found; their common feature is an M-fold modulation of the twist angle over the supercell period, with M smaller than N and generally not a simple fraction of it. The global minimum was found to conform to the ratio $k = M/N = 6/14$, which is close to the experimentally observed $k = 6/13$ in the incommensurate phase III. Enthalpy minimization showed an overall decrease in the magnitude of the twist angle down to $\tau \simeq 0^\circ$, as well as the evolution of the modulated structures towards the high-temperature structure with increasing pressure, in agreement with evidence for the high-pressure limit of the incommensurate biphenyl phases.

1. Introduction

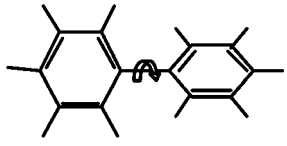

Biphenyl is a classic example of a molecule whose conformation is influenced by crystal packing. This molecule consists of two phenyl rings connected by a single C—C bond, around which rotation by the angle τ can occur. Its conformation is determined by two competing factors: the π-electron effect that favors coplanarity of the phenyl rings and the nonbonded

contacts between the H atoms in the *ortho* positions that form unusually short van der Waals H···H distances, if $\tau = 0$. In the gas phase the molecule is nonplanar, with $\tau \simeq 45^\circ$ (Almenningen *et al.*, 1985), whereas in the room-temperature crystal the molecule adopts, at least on average, a perfectly planar shape because of its location on the centrosymmetric position of space group $P2_1/c$ ($Z = 2$). At low temperature structural transitions into phases II and III take place at 42 and 17 K in biphenyl (38 and 24 K in biphenyl-d_{10}), respectively, where the crystal structure loses the center of symmetry while the molecule returns to a nonplanar shape (Bree & Edelson, 1978). The full crystal structure of biphenyl-d_{10}, studied by neutron diffraction at 22 K, was initially described as a noncentrosymmetric superstructure (space group Pa, $Z = 4$). This results from doubling the cell period b of the high-temperature phase I, in which the molecule retains its principal position and orientation while its shape is no longer planar but is twisted by $\sim 10^\circ$ (Cailleau *et al.*, 1979). Such a structure (referred to as the 'basic structure', see Fig. 1), however, turned out to be only approximate as subsequent high-resolution inelastic neutron scattering studies (Cailleau, 1986) proved both low-temperature phases to be incommensurate. Thus, the phase II modulations are characterized by a wavevector **q** of some general direction and magnitude in (**a***, **b***, **c***) space (but rather close to **b***); its components change gradually with temperature (Cailleau *et al.*, 1986). In phase III a partial 'lock-in' transition (restoration of periodicity) takes place in the modulations characterized by $\mathbf{q} \simeq 6/13\mathbf{b}^*$ (Cailleau, 1986). The structure refinement of phase III (Baudour & Sanquer, 1983) showed the major component of the structure modulations to be periodic changes in the twist angle of the molecule approximated by a sine wave with the maximum amplitude $\tau_{max} = 11^\circ$.

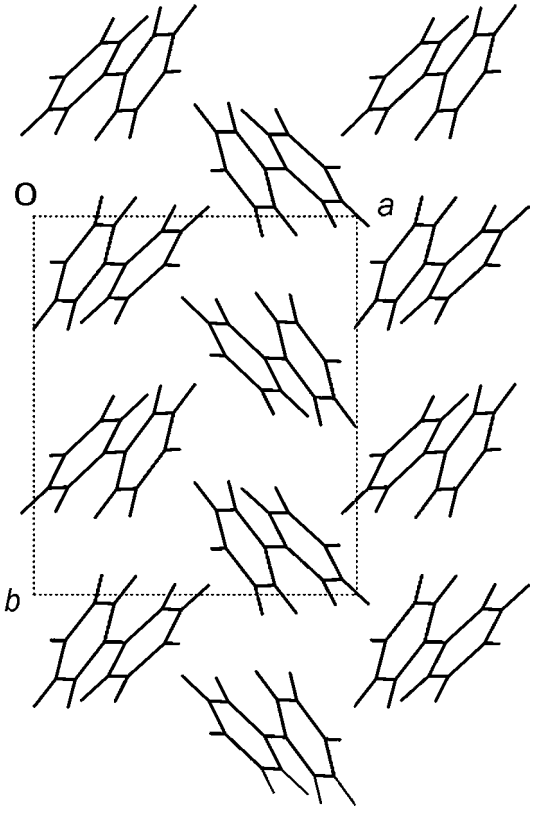

Figure 1
View of the basic structure of biphenyl showing the molecules arranged in a densely packed *ab* layer, in which their axes are nearly parallel to each other and inclined at $\sim 75^\circ$ to the layer plane. The rows of cooperatively twisted molecules run along *b*.

Previous theoretical work on solid biphenyl involved the interpretation of the incommensurate phase transitions within the framework of phenomenological Landau theory (Ishibashi, 1981; Ecolivet *et al.*, 1983; Parlinski *et al.*, 1989; Launois *et al.*, 1989). A purely Landau treatment was completed with a microscopic physical model of 'frustrated' molecular twists (Heine & Price, 1985; Benkert *et al.*, 1987). Lattice-dynamical calculations (Takeuchi *et al.*, 1981; Natkaniec *et al.*, 1981; Plakida *et al.*, 1983) have shown the occurrence of a strong coupling between the intramolecular torsional and intermolecular translational modes that results in a soft-mode behavior away from the boundary of the Brillouin zone, indicative of a commensurate–incommensurate phase transition. The effect of crystal packing on the conformation of the biphenyl molecule was modelled by minimization of the lattice energy with atom–atom potentials to account for the nonbonded energy and an empirical torsional potential of simple shape to describe the π-conjugation effect (Casalone *et al.*, 1968; Brock, 1979; Busing, 1983; Corish *et al.*, 1995). While the previous authors based their models on the observed crystal structures, no attempts were made to apply them in the prediction of the biphenyl phases *ab initio* without prior knowledge of the experimental crystal data. In this paper we conduct such an attempt with global lattice-energy minimization in the various structural classes most likely in organic crystals. We also characterize the landscape of the potential energy in the region of the low-temperature phase transition. Further, the nature of the incommensurate state of biphenyl is studied by the energy minimization of a series of quasi-one-dimensional superstructures built of N unit cells of the high-temperature structure, with N varied as a discrete parameter. Finally, the simulated biphenyl structures involved in the phase transition are characterized in terms of their behavior under pressure.

2. Details of the calculation

The biphenyl molecule was modeled as a flexible system composed of two phenyl fragments with fixed geometry. Each phenyl ring had perfectly hexagonal (D_{6h}) geometry with the C—C bond length 1.397 Å. The C—H distance was shortened to 1.027 Å, as required by the potential parameters of Williams & Starr (1977) that were used in this work. The standard geometry around the central C—C bond was maintained by bond-variation potentials of the quadratic form (Table 1).

With the present phenyl geometry, the closest intramolecular H···H distance of the *ortho* H atoms is 0.06 Å shorter than the distance (1.93 Å) experimentally observed by

Table 1
Bond-variation potentials of the type $V_{bv} = w(d - d_0)^2$ used to maintain standard geometry of the biphenyl molecule around its central bond.

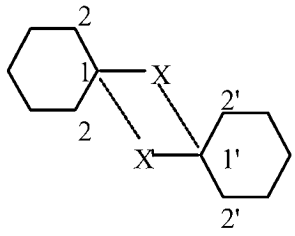

C1: atoms of the central bond, C2: atoms next to C1; X is an auxiliary force center associated with the phenyl ring (distances C1$-X$ and C1′$-X'$ are 1.50 Å, angles C2$-$C1$-X$ and C2′$-$C1′$-X'$ are 120°), *i.e.* X geometrically coincides with the C1 of the *other* phenyl ring in an undistorted molecule with the C1$-$C1′ distance being exactly 1.50 Å.

Interaction	d_o (Å)	w (kJ mol^{-1})
C1$\cdots X'$ and C1$\cdots X$	0.00	2093
C1$\cdots$C1′	1.50	2093
C1$\cdots$C2′ and C1′$\cdots$C2	2.52	837

neutron diffraction in the planar biphenyl molecule (Baudour *et al.*, 1986). Nevertheless, such a contraction is not that critical to our model because the central C$-$C bond length is flexible; its actual length (and hence the intramolecular H$\cdots$H distance) is self-regulated in the equilibrium structure by the total balance of the competing intra- and intermolecular forces.

The potentials of the exp-6-1 type [$A\exp(-Br) - C/r^6 + q_iq_j/r$; Williams & Starr, 1977] were used to describe the nonbonded interactions of the van der Waals and electrostatic types for pairs of atoms belonging to different phenyl rings in the same molecule and in different molecules (Table 2). These potentials have proven to be capable of reproducing the observed structure of benzene as the global minimum correctly (Dzyabchenko, 1984*a*,*b*; Gibson & Scheraga, 1995; van Eijck *et al.* 1998). The torsional potential to describe the π-stabilization effect had the form

$$V_{el}(\tau) = V_\tau(1 - \cos^2 \tau), \quad (1)$$

where the constant V_τ was obtained by adjusting the solid-state twist angle of the molecule to the experimental value, as described in §3.1.

In the calculation of the slowly converging lattice-energy sums of the terms with r^{-6} and r^{-1}, the accelerated convergence method was used (Williams, 1971; Dzyabchenko & Agafonov, 1995). The convergence constant K was taken as 0.175 Å^{-1}. With this choice of K, the contribution of the reciprocal lattice sums (E_r) to the total energy does not influence the positions of the energy minima markedly and E_r was ignored in the local minimizations to reduce the computational costs. However, for the final energy ranking E_r was calculated once for the minimized structure and added to the minimized energy as a correction term. Table 3 presents a test of the accuracy of the lattice energy summation for a few biphenyl structures to be discussed in subsequent sections. It can be seen that while a change in K from 0.175 to 0.300 Å^{-1} results in significant changes in both the direct- and reciprocal-lattice energy contributions to the dispersion and Coulombic energy, their sums remain constant within at least 0.0001 kJ mol^{-1}, thus indicating that the lattice summation is complete.

Table 2
Nonbonded exp–6–1 potentials [$A\exp(-Br) - C/r6 + q_iq_j/r$] used for modeling biphenyl structures (Set II of Williams & Starr, 1977).

Energies are in kJ mol^{-1}, lengths in Å. Charges on atoms are 0.153 e for H atoms and -1.53 e for the C atoms of the ten C$-$H groups, and zero for the two C atoms of the central C$-$C bond; r_o and u_o are the equilibrium distance and potential-well depth, respectively.

Interaction	A	B	C	r_o	u_o
H$\cdots$H	11 680	3.74	136	3.297	−0.054
H$\cdots$C	65 480	3.67	573	3.601	−0.143
C$\cdots$C	367 200	3.60	2414	3.900	−0.392

In local minimization, each phenyl fragment moved in the field of nonbonded bond variation and torsional potentials independently of other such fragments comprising the asymmetric unit, with an allowance for the three translational and three rotational degrees of freedom. Each minimization was carried out in a few steps: in each step a perfectly smooth (with a fixed list of atom pairs taken into consideration throughout the step) function F, which approximated the actual energy function E, was minimized; in the final steps the minimum of F converged to the minimum of E (Dzyabchenko & Agafonov, 1995). The energy calculations were carried out with the program *PMC* (Dzyabchenko, 2001), in which later modifications were made to include the torsional potential and automatic generation of grid points.

2.1. Global minimization strategies

Global minimization was carried out in two ways. The first was a systematic grid search using the structural classes most likely for organic crystals. A structural class is indicated by the space group, the number of molecules per unit cell (Z) and the orbits occupied by the molecules. The structural class specifies the topology of a crystal packing more definitively than the space group alone. Statistical data on the occurrence of various structural classes in organic homomolecular crystal structures are available (Belsky *et al.*, 1995). They provide an empirical basis for selecting structural classes in the crystal structure predictions in a rational way (Dzyabchenko, 1984*a*; Dzyabchenko *et al.*, 1996; van Eijck, 2002).

Table 4 lists the structural classes used in the generation of biphenyl structures with the molecule(s) in a general position (not on a crystal symmetry element). For monoclinic groups, two unit-cell settings were adopted – the standard c-glide and an alternative n-glide – to avoid the necessity for starting structures with large monoclinic β angles. Assuming the convergence ranges observed regularly for the monoclinic angle in the minimization results, we found it safe enough to restrict the variety of the starting cells to the rectangular cells only. While the majority of classes of Table 4 assume only one independent molecule in a general position, the groups $P2_1/c$, $P2_1$, $P\bar{1}$ and $P1$ were also allowed to have two independent

Table 3
Test calculations on the slowly converging lattice sums in biphenyl structures.

E_{6d} and E_{1d} are direct-space sums of the dispersion and Coulombic energy; E_{6r} and E_{1r} represent the reciprocal-space parts neglected during local minimization, but used as correction terms to the minimized energies.

Structure	High-temperature		Basic		6/13		6/14	
K_{conv} (Å^{-1})†	0.175	0.3	0.175	0.3	0.175	0.3	0.175	0.3
E_{6d}	−189.9635	−154.5130	−185.7524	−149.5127	−186.6852	−150.6310	−186.6316	−150.5992
E_{6r}	−0.3915	−35.8419	−0.4040	−36.6437	−0.4049	−36.4591	−0.4040	−36.4365
$E_{disp} = E_{6d} + E_{6r}$	−190.3549	−190.3549	−186.1564	−186.1564	−187.0901	−187.0901	−187.0357	−187.0357
E_{1d}	−11.6179	−39.2064	−11.8528	−39.5673	−11.8507	−39.5489	−11.8302	−39.5397
E_{1r}	2.2249	29.8133	2.2831	29.9976	2.2931	29.9913	2.2948	30.0043
$E_{Coul} = E_{1d} + E_{1r}$	−9.3931	−9.3931	−9.5698	−9.5698	−9.5576	−9.5576	−9.5354	−9.5354

† The convergence constant in the expressions for the accelerated convergence method (Williams, 1971). The cutoff parameters in this test are 12 Å and 1.5 Å^{-1} for the direct and reciprocal space, respectively.

Table 4
Structural classes and starting cell shapes used in the global minimization.

The left column lists the most likely structural classes with one and two independent molecules in general positions, selected according to Belsky *et al.* (1995). Groups in parentheses complement the monoclinic groups with an alternative choice of unit cell axis in the *ac* plane (see text). The symbols C, F, T, L and W represent 'cubic', 'flat', 'tall', 'long' and 'wide' cell shapes, respectively, as described in the text.

Structural classes	Cell shapes
$P1$, $Z = 1$ and 2; $P\bar{1}$, $Z = 2$ and 4; $P2_12_12_1$, $Z = 4$; $Pbca$, $Z = 8$	C, F, T
$P2_1$, $Z = 2$ and 4 ($I2$, $Z = 4$; Pn, $Z = 2$ and 4; $P2_1/n$, $Z = 4$ and 8)	C, F, T, L
Pc, $Z = 2$ and 4; $P2_1/c$, $Z = 4$ and 8; $C2$, $Z = 4$; Cc (Cn, Ic) $Z = 4$; $Pna2_1$, $Z = 4$; $Pca2_1$, $Z = 4$; $C2/c$ ($C2/n$, $I2/c$), $Z = 8$	C, F, T, L, W

molecules in the asymmetric unit: these three classes amount together to 6.5% of the total number of organic homomolecular structures as compared with some 11% for all classes with more than one independent molecule (Belsky *et al.*, 1995). The class Pc, $Z = 4$, was also added to the list of structures as the experimentally observed one. The classes with the molecule occupying a crystallographic symmetry element (special-position classes) were not considered specially, since such classes are implicitly present in some of the general-position classes of Table 4. With the abundance of the special-position classes taken into account, we find (with the data of Belsky *et al.*, 1995) that the structural classes of Table 4 cover ∼91% of the total abundance of the organic structural classes.

The starting cell dimensions were confined to a few rectangular ($\alpha = \beta = \gamma = 90^\circ$) cell shapes: 'cubic' ($a = b = c = x$), 'flat' ($a = x2^{1/2}$, $b = x/2$, $c = x2^{1/2}$), 'tall' ($a = c = x/2^{1/2}$, $b = 2x$), 'long' ($a = 2x$, $b = c = x/2^{1/2}$) and 'wide' ($a = b = x/2^{1/2}$, $c = 2x$). Here, the magnitude of x was chosen so that x^3 would be greater by 25–50% than the anticipated unit-cell volume to reduce the probability of occurrence of physically meaningless short distances in the starting structure. Further, depending on the space group, some of these shapes were omitted by symmetry (Dzyabchenko, 1983). In the event that the minimization failed in a few initial steps, the same starting point was repeatedly attempted with the starting cell dimensions increased each time by a few per cent. The starting molecular shape was taken as planar. The starting sets of Euler angles φ, θ, ψ were selected with a 30 ° increment in each angle to give 168 unique orientations in the range $-\pi/2 > \varphi > \pi/2$, $0 > \theta > \pi/2$, $0 > \psi > \pi$, consistent with the D_{2h} point group of the molecule in the planar state. The starting values of each of the three translational parameters of the molecule were 0 and $\frac{1}{4}$, yielding in total the eight corners of an $a/4 \times b/4 \times c/4$ box, the asymmetric unit of the Cheshire-group cell (Hirshfeld, 1968).

An alternative (second) strategy for carrying out the global minimization was sampling the configurational space of the $P1$ group with the Z molecules allowed to move independently (Dzyabchenko, 1987, 1989; Gibson & Scheraga, 1995). For a reasonably large Z this approach is barely affordable in a $6Z$-dimensional grid search with sufficiently small steps, unless some hypothesis (such as the use of a trial space group) is introduced to connect the positions and orientations of the Z molecules at the start. Thus, Gibson & Scheraga (1995) used the experimental space group $Pbca$ in the generation of starting structures of benzene optimized in $P1$ with four independent molecules. The rationale for using space groups in this way is to create uniform distributions of the positions and orientations of the Z molecules in the three dimensions compatible with crystal periodicity. In this work, we considered the case of $P1$, $Z = 8$, since $Z > 8$ is a rare case with organic structures (1.7% according to Table 3 of Belsky *et al.*, 1995). Rather, it totally excludes the trigonal and hexagonal structures (2.7%) since $Z = 8$ is not compatible with these symmetries. The grid set for a first independent molecule was the same as before (8 translations combined with 168 orientations), while the starting positions and orientations of the other seven molecules were generated by the operators of the space groups $F\bar{1}$, $C2/c$ and $Pbca$, thus arranging the eight molecules in one, two and four different orientations, respectively. The latter two groups were selected because they are most common for $Z = 8$ (Belsky *et al.*, 1995). The starting cell shapes were assigned in the same way as in the case of one independent molecule (Table 4) and $F\bar{1}$ was treated as $P\bar{1}$.

The energy-minimized structures were sorted by energy and compared with each other with the aid of the program *CRYCOM* (Dzyabchenko, 1994) to give the list of unique structures. Finally, each unique structure was examined with *CRYCOM* once again to characterize its actual lattice type, the space group, conventional-cell dimensions and the site-symmetry element(s) if present.

Table 5
Comparison of the observed and calculated structures of biphenyl.

Observed: high-temperature form at T = 110 K (Charbonneau & Delugeard, 1976) and 293 K (in parentheses; Charbonneau & Delugeard, 1977). Low-temperature form: T = 22 K (Cailleau *et al.*, 1979). The 'preliminary model', Table 2 of Busing (1983), is given in column two.

	Observed	Calculated by Busing	Calculated in this work
High-temperature form, $P2_1/a$, Z = 2			
a (Å)	7.82 (8.12)	8.06	8.07
b (Å)	5.58 (5.63)	5.49	5.51
c (Å)	9.44 (9.51)	9.30	9.33
β (°)	94.6 (95.1)	90.3	90.5
V/Z	205.3 (216.1)	205.8	207.4
τ_1 (°)	0 (0)	0.0	0.0
θ (°)†	0 (0)	4.1	0.1
Low-temperature form, Pa, Z = 4 (the basic structure)			
a (Å)	7.77	8.15	8.15
b (Å)	11.14	10.90	10.95
c (Å)	9.44	9.32	9.38
β (°)	93.7	90.8	91.3
V/Z	203.8	207.0	209.0
τ_1 (°)	10.2	10.2	11.1
τ_2 (°)	−10.2	−10.3	−11.1
θ_1 (°)†	0	2.7	1.4
θ_2 (°)†	0	2.6	0.1

† Net rotation angle which relates the molecular orientation of the predicted structure to the experimental one.

Energy calculations were carried out on a cluster of PC computers, Pentium III and AMD Athlon, running under Linux. Typical execution times (on a Pentium III computer with a single 1 GHz processor) ranged from a few seconds for one starting point in the case of one independent molecule to about 2.5 min for the superstructures with N = 16. The total computational expense (referred to a Pentium III 1 GHz processor) amounted to ∼1070 h, of which 30 h were consumed for the 19 structural classes with one independent molecule (∼32 000 starting points), 270 h for the five classes with two independent molecules (161 000 starting points), 330 h for the $P1$, Z = 8 case (20 000 starting points) and 440 h for the N-fold superstructures with N ranging from 4 to 16 (20 000 starting points).

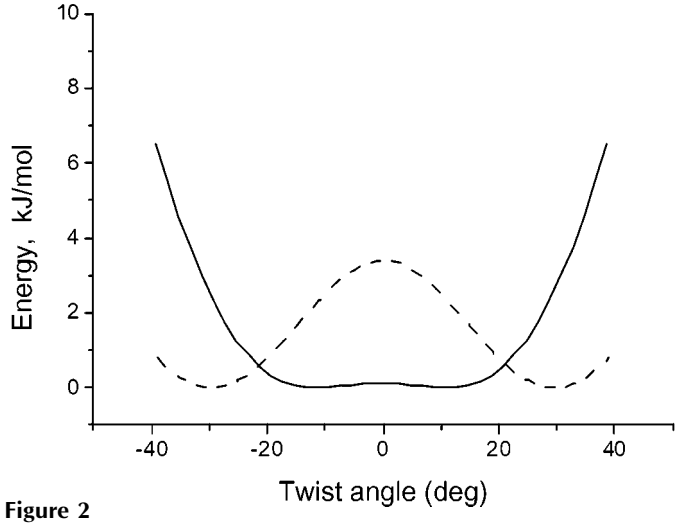

Figure 2
Solid line: dependence of the lattice energy ($E = E_{pack} + E_{conf}$) of biphenyl on the twist angle τ_1 of one molecule, while the conformations of three other independent molecules as well as the six lattice constants are optimized in $P1$, Z = 4. The dashed line shows the conformational energy E_{conf} contributing to the total lattice energy E.

3. Results and discussion

3.1. Adjustment of torsional potential

A series of trial minimizations with various values of the torsional constant in (1) resulted in V_τ = 67.0 kJ mol^{-1} as the best one to reproduce the observed nonplanar shape of biphenyl in the basic structure of the low-temperature phase (Cailleau *et al.*, 1979), approximating the actual incommensurate structure (Baudour & Sanquer, 1983). This value of V_τ was used throughout all of this work. The minimized structures of both the high- and the low-temperature phases are compared with the experimentally observed structures in Table 5. It can be seen that the agreement of the minimized structure with the experimental one is very good except for the unit-cell parameter a, which is sensitive to changes in temperature. Our results are almost identical to the 'preliminary model' of Busing (1983), which demonstrates the same trends in the calculated structures.

The energy profile of the twist rotation τ of the isolated biphenyl molecule, calculated with the same V_τ, has a characteristic double-minimum form with $\tau_{opt} = 29°$ and the height of the potential barrier is 6.7 kJ mol^{-1}. The corresponding experimental gas-phase values are $44 \pm 1°$ and 9.2 kJ mol^{-1}, respectively (Almenningen *et al.*, 1985). It should be noted that these data refer to a rather high temperature (∼400 K), where intense thermally activated intramolecular vibrations (in particular, the in-plane molecular bends) increase the effective size of the phenyl *ortho*-H atoms, which in turn should result in increasing the observed twist angle. On the other hand, *ab initio* calculations for the isolated molecule (Tsuzuki *et al.*, 1999) predict twist angles rather close to the experimental value. At any rate, we believe that the addition of a second term, $V'_\tau(1 - \cos^2 2\tau)$, to the torsional potential V_{el}, with a proper choice of V'_τ, would improve the agreement of the gas-phase conformation with little influence on the solid-state results because the latter results are based on the behavior of V_{el} in the vicinity of $\tau = 0$ and are rather insensitive to its details at large twist angles.

3.2. Energy profile and barrier to twist rotation in the solid state

The calculations of the energy profile were carried out in the following way. The lattice energy of the basic structure was minimized in $P1$, Z = 4, and the cell dimensions and all parameters of the four independent molecules were varied independently, except for the twist angle (τ_1) of the first molecule; τ_1 was altered stepwise in successive minimization runs with a small increment. It was found that the optimized twist angle (τ_2) of another molecule, adjacent to the first one in the same b row, changed synchronously with $-\tau_1$ all the way through the stationary point at $\tau_1 = \tau_2 = 0$ and up to a

Table 6
Energies and structural parameters of the predicted biphenyl structures.

T4: the number of molecules and cell dimensions refer to a *B*-centered pseudomonoclinic cell with $\alpha \simeq -\gamma \simeq -90^\circ$ (see also Table 7).

Structure name	High temperature	T4	Basic	6/13	6/14
Space group	$P2_1/a$	$P\bar{1}$	*Pa*	*Pa*	*Pa*
Z	2	8	4	26	28
N	1	2	2	13	14
Energy (kJ mol^{-1})	0.20	0.14	0.00	−0.03	−0.09
Cell parameters (Å, °):					
a	8.07	16.30	8.16	8.16	8.18
b/*N*	5.51	5.47	5.46	5.47	5.46
c	9.33	9.36	9.38	9.41	9.36
β	90.5	91.0†	91.3	91.4	91.4
D, g/*cm*3	1.235	1.228	1.224	1.222	1.224

† See headnote.

Table 7
Biphenyl structures of the space group $P\bar{1}$ built of centrosymmetric rows.

Z: Number of molecules in the primitive cell; supercell: Bravais type of centering and the parameters of the pseudomonoclinic ($\alpha \simeq \gamma \simeq 90^\circ$, $\beta \simeq 91^\circ$) supercell of the triclinic lattice in terms of the *a*, *b* and *c* unit-cell parameters of the basic structure.

Structure	Energy (kJ mol^{-1})	*Z*	Supercell	⟨*τ*⟩ (°)
T1	0.08	8	*A*: *a*, *b*, 4*c*	13
T2	0.11	8	*B*: 2*a*, *b*, 2*c*	10
T3	0.12	8	*P*: *b*, *a*, 2*c*	11
T4	0.14	4	*B*: 2*a*, *b*, *c*	9
T5	0.25	4	*F*: 2*a*, *b*, 2*c*	7

symmetry minimum where both angles adopted the values that they had in the initial state but with opposite sign ($\tau_1 = -11^\circ$, $\tau_2 = 11^\circ$). At the same time, the twist angles τ_3 and τ_4 of the other two molecules, constituting another row, remained virtually unaffected. This behavior is a consequence of close intermolecular contacts within a tightly bound *ac*-layer (Fig. 1). Hence, the phenyl groups in the same-row pair of molecules contact each other with their lateral edges, thus effectively clutching one another. On the contrary, in a closest contact between the rows, the phenyl edge of one molecule points close to the central axis of the other molecule, and the two phenyls together thus form a T-shaped configuration in which the mutual influence of phenyl rotations is small.

Fig. 2 shows the calculated energy profile, with two shallow minima separated by a potential barrier of ∼0.13 kJ mol^{-1}. At the top of the potential barrier, the structure contains the *b* rows of planar molecules ($\tau_1 = \tau_2 = 0$) alternating in the *a* direction with rows of twisted molecules ($\tau_3 = -11^\circ$, $\tau_4 = 11^\circ$). To the left of this point there is an energy well of the basic structure, while the well to the right represents a structure, in which one *b* row consists of the twisted molecules inverted about their mass center. (The latter structure is an actual energy minimum and thus represents a hypothetical biphenyl polymorph.) Another series of the τ_1-fixed minimizations was carried out under *Pa* symmetry constraints. This symmetry imposes a synchronous change of the twist angles in the different *b* rows, while they remain independent in the same row. Nevertheless, the optimal τ_2 values were found to be identical with $-\tau_1$. The resulting profile is similar to that of Fig. 2, while the height of the energy barrier ΔE increases to 0.20 kJ mol^{-1}, the energy difference between the basic and the high-temperature structures (Table 6). On account of our simulation results on the high-order superstructures (§3.4), in which the experimentally observed 6/13 structure representing phase III was found to be 0.03 kJ mol^{-1} lower than that of the basic structure, the calculated height of the high-temperature structure over the ground state is 0.23 kJ mol^{-1}. Such a low height is consistent with the idea that the large-amplitude thermal vibrations stabilize phase I in a free-energy minimum above some critical temperature. The estimation of this temperature as $T_c \simeq \Delta E/k_B \simeq 30$ K agrees in order of magnitude with the experimentally observed phase transition temperatures $T_{\mathrm{I–II}}$ and $T_{\mathrm{II\text{-}III}}$. A more detailed consideration of the low-temperature phase transition mechanism in biphenyl, as well as our proposals concerning the structure of phase II, will be presented elsewhere.

One more principal result of the present section is the observation that the conformational changes of the molecules within a *b* row are highly cooperative, whereas such changes in different *b* rows do not influence each other. Moreover, a simultaneous change of the signs of the twist angle within a *b* row (resulting in its inversion about the midpoint of the central C—C bond of a biphenyl molecule) produces a new structure with nearly the same energy as the original structure.

3.3. Global search results ($Z \leq 8$)

The global search did not find any structures with lower energy than that of the basic structure taken as zero. The structural classes with one independent molecule produced either the high-temperature structure or a yet higher energy one in the lowest minimum. As indicated above, the high-temperature structure is a stationary point in the energy function rather than a minimum. It frequently occurs, however, that stationary points occur as minima in structure-simulation results due to the space-group symmetry constraints (Dzyabchenko, 1989). Specifically with biphenyl, it was the translational symmetry with a short (∼5.5 Å) cell dimension that stabilized the high-temperature structure as an energy minimum. The same occurred with many other structures of yet higher energy than the high-temperature one, where such a short period occurred as one of the lattice dimensions. Moreover, some portion of the minimized structures with no such 5.5 Å period also turned out to be stationary points (or very shallow minima), which was revealed during additional minimization in *P*1. With all such artifact solutions eliminated, the rest of the structures were found to be rather high in energy (energy of the basic structure is accepted as zero): the most stable of them was 3.8 kJ mol^{-1} (in the class *Pbca*, $Z = 8$).

The search in the classes with two independent molecules, except for $P\bar{1}$, showed a similar picture: there were either artifact minima with a short cell dimension or true minima of high energy (the lowest was of 1.7 kJ mol^{-1}, $P2_1/n$, $Z = 8$). The

basic structure has been observed many times in *Pc* (*Pn*), Z = 4. Thus, of some 2500 events of energy minima lower than 5 kJ mol^{-1} reached in *Pc*, Z = 4, one quarter corresponded to the basic structure, 70% were artifact minima with $a \simeq 5.5$ Å, while the remainder were more than 2.7 kJ mol^{-1} higher in energy. In contrast, the search in $P\bar{1}$, Z = 4, resulted in a few low-energy structures (T4 in Table 6; T4 and T5 in Table 7).

The *P*1, Z = 8, search yielded 150 unique structures of energy lower than 5 kJ mol^{-1} originating from 570 starting points. (This is quite a small fraction of a total of 18 000 starting points yielding minimized structures of less than 50 kJ mol^{-1} in energy.) Part of them were, again, artifact minima with $a \simeq 5.5$ Å, while 105 were recognized as stable. Only three of them were of lower energy than the high-temperature structure (Table 7), but still higher than the basic structure. With the aid of *CRYCOM*, various space groups were identified in the list of 105 unique structures. Thus, $P\bar{1}$, $P2_1/c$, *Pc*, $P2_1$, *Pbca*, $Pca2_1$, $Pnc2_1$ and $P2_12_12$ were detected within the Z = 8 cells; three $P\bar{1}$ and one *P*1 structures had cells which were half the size. Still, the major part of the structures had no symmetry other than *P*1 with the triclinic Z = 8 cell. While differing in symmetry and exact geometrical details, the biphenyl structures (E < 5 kJ mol^{-1}) exhibit remarkable similarity in their principal architecture. In particular, dense molecular layers and cooperative rows of generally nonplanar molecules were found in all structures. The rows had a periodicity of ∼11 and ∼22 Å. The twist angles had a general tendency to increase in absolute value for the higher-energy structures (up to 25° at the level of ∼5 kJ mol^{-1}). Within a row of ∼11 Å, the twist angles of adjacent molecules were found to be identical in the absolute value and opposite in sign as in the basic structure; at the same time they could differ in absolute value if they occurred in different rows. Some structures containing rows of ∼22 Å admit $|\tau|$ to being different in the same row, but their energy was relatively high.

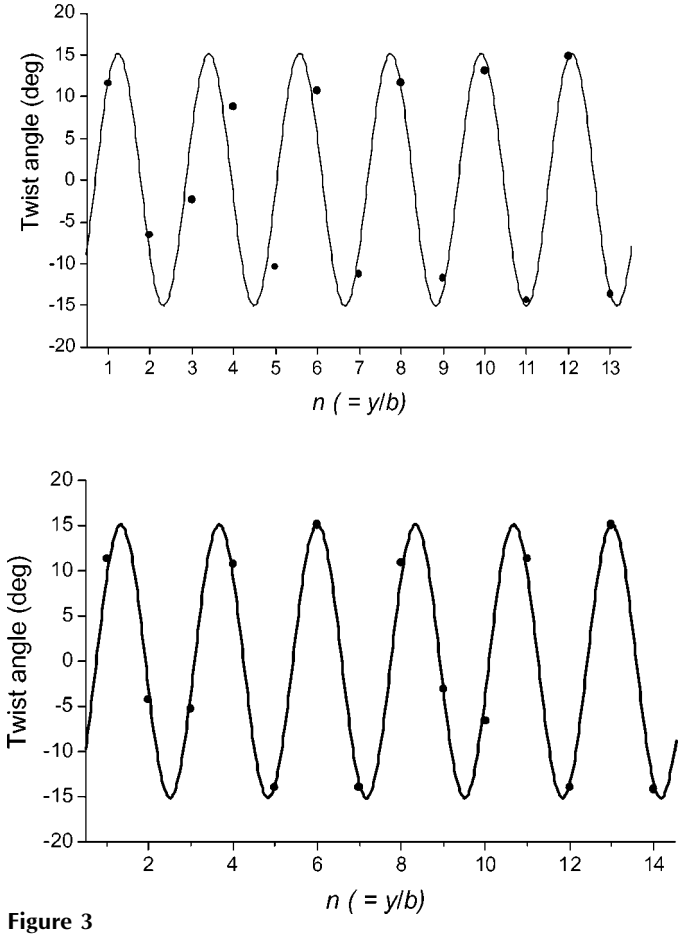

Figure 3
Twist-angle modulation in the superstructures 6/13 (top) and 6/14 (bottom). Filled circles represent the magnitudes of the twist angles found in the energy-minimized structures, plotted against the y coordinates of the molecules (b is the cell dimension of the high-temperature structure). The curves are analytical functions $\tau(y) = \tau_m \sin(2\pi yM/Nb + \varphi_0)$, fitted to the modulation wave: $\tau_{max} = 15°$, M = 6, N = 13 and 14, φ_0 = 0.74 and 0.76, respectively, for the first and the second plots.

Several lowest-energy structures found in *P*1, Z = 8, presented in Table 7 (two of them, T4 and T5, are the same as those found in $P\bar{1}$, Z = 4), are centrosymmetric with nonplanar molecules in a general position. The structures have pseudo-monoclinic lattices that are remarkably close to the basic structure lattice: the respective relationships are best characterized by their centered supercells, whose parameters are multiples of the cell parameters of the basic structure (column 4 of Table 7). The positions and orientations of the molecules as a whole are very similar as well. Moreover, rows of cooperatively twisted molecules in the $P\bar{1}$ structures are centrosymmetric: each two adjacent molecules in a row are related through an inversion center of the crystal, while such molecules in the basic structure are not related through any symmetry element. On the other hand, no symmetry elements connect the neighboring rows in the layer of a $P\bar{1}$ structure, in contrast to the basic structure in which rows are connected through the glide plane. Generally, while being almost identical in the crystal packing and the molecule conformation, these lowest-energy structures are principally different if one looks at the patterns of the signs of the twist angles of the respective molecules.

As noted above, the yield of low-energy (< 5 kJ mol^{-1}) structures of the total number of starting points is insufficient to guarantee that the final list of the *P*1, Z = 8, structures be exhaustive. (Thus, the basic structure itself has never occurred in this search). At the same time, the noted structural similarities allow us to suggest that the missed structures are essentially identical to those actually found. Moreover, it is possible to expand the list of structures on the basis of those known. Actually, as found in §3.2, by cooperatively changing the τ signs of the molecules forming a b row, a new structure results with no significant change in the energy or in the optimized structure parameters. Therefore, doing so with selected rows of the unit cell (or a supercell, extended in the directions normal to the row direction) presents the opportunity to list the derivative structures in a systematic way. Thus, changing the signs in any two subsequent b rows along the a axis of the basic structure results in structure T4. *p*-Terphenyl (Ph—C_6H_4—Ph) and *p*-quaterphenyl (Ph—C_6H_4—C_6H_4—Ph), the analogues of biphenyl in the polyphenyl family, are isostructural with biphenyl at room temperature

and, in analogy with biphenyl, exhibit phase transitions with a conformational change and unit-cell doubling at low temperatures (Baudour *et al.*, 1976; Delugeard *et al.*, 1976; Baudour *et al.*, 1978). However, these low-temperature structures are centrosymmetric, with the space group $P\bar{1}$ (Z = 4), in contrast to the monoclinic group *Pa* in the low-temperature biphenyl. At the same time, there are supercells in both structures with pseudomonoclinic cell dimensions, which show the relationship $a \simeq 2a'$, $b \simeq 2b'$, $c \simeq c'$, $\beta \simeq \beta'$ with the unit cells of the respective high-temperature structures. In this connection we note that the T4 cell demonstrates the same relationship to the high-temperature cell of biphenyl. While the *p*-terphenyl structure is disordered and difficult to analyse, quaterphenyl demonstrates an obvious structural similarity to T4. Actually, with the aid of *CRYCOM*, we found a correspondence in the arrangement of the four independent phenyl fragments in T4 with the respective fragments in the low-temperature quaterphenyl structure (Baudour *et al.*, 1978): the r.m.s. deviations are 0.08 Å and 11° for phenyl translations and rotations, respectively. (Note that the major fraction of the 11° disagreement in the phenyl rotation is caused by an overall rotation of the molecules in the two structures, while there is correspondence in the magnitudes and signs of the twist angles of the respective molecules). By analogy, it may therefore be proposed that a metastable polymorph of *p*-quaterphenyl exists, with its structure symmetry (*Pa*, Z = 4) being similar to the basic structure of biphenyl.

3.4. Superstructure simulations

The nature of the incommensurate phases is the most intriguing part of the biphenyl problem. With the aim of modeling the quasi-one-dimensional incommensurate phase III of biphenyl, energy minimizations were carried out for a series of biphenyl superstructures whose supercells were N unit cells of the high-temperature structure along the b direction. The space group *Pa* experimentally observed in phase III (Baudour & Sanquer, 1983) was imposed in these calculations. The variable parameters were therefore the four cell dimensions of the monoclinic cell and the 12N rigid-body parameters of the 2N phenyl fragments. In searching for energy minima, we first tried various random sets of τ values deviating by no more than 11° of its absolute value. It was soon realised that low energies are associated with such distributions of twist angles $\tau_1, \ldots \tau_N$ over the N successive molecules that conform to a periodic function, the M folds of which match the supercell period. Consequently, we switched to the strategy in which sets of starting twist angles were generated according to

$$\tau_n = \tau_{\max} \sin(2\pi n M/N + \varphi), \qquad (2)$$

where $\tau_{\max}$ is the maximum amplitude 11° and n is the sequential number of a molecule (n = 1, 2, ..., N). The wavenumber M and initial phase φ were changed stepwise to obtain grids of starting models. With N even, all combinations of M and N resulting in $k = M/N = 1/2$ were rejected as representing the basic structure. It was also found helpful for successful optimization to induce small initial shifts of the center-of-mass coordinates of the biphenyl molecules away from the b row axis in the a and c directions. Such shifts were also generated with (2), with $\tau_{\max}$ replaced by the respective maximum amplitudes $\Delta x_{\max} = 0.003$ and $\Delta z_{\max} = 0.005$ (φ is zero here since, with the *Pa* space group, it does not influence the structure). We stress that (2) described only the starting parameter sets, but that no parameters of the 2N phenyl fragments were constrained in the subsequent minimization. Moreover, the final characteristics of the modulation wave (as obtained from fits of a sine function to the distributions of τ angles in the optimized structures) were usually completely different from the starting parameters $\tau_{\max}$, M/N and φ.

The search resulted in a number of superstructures of lower energy than that of the basic structure. Their common feature is the presence of N molecules along the b direction of the supercell in conformations given by a sequence of twist angles, τ that fit reasonably closely to a sine function whose periodicity was distinct from the supercell period $bN = Nb$. Fig. 3 shows plots of the twist angles found in the simulated superstructures with k = 6/13 and 6/14, as well as the sine functions fitted to these angles by least-squares. As noted above, small periodic shifts in the x and z coordinates of the centers-of-mass of the biphenyl molecules from their average positions were also an essential feature of the simulated superstructures (while no such modulation was found in the y coordinates). The periodicity of these displacements was quite different from that of the twist angles. Thus, in the 6/13 structure the x-coordinate modulation wave contained one peak per supercell period with a maximum amplitude of 0.01 as compared with two peaks with amplitudes nearly half the size in the 6/14 structure.

Fig. 4 presents the lattice energies of the superstructures plotted against the twist-angle modulation wavelength $\lambda/b = N/M = 1/k$, where M is the number of folds of the modulation wave in the sine-function fit to the distribution of twist angles

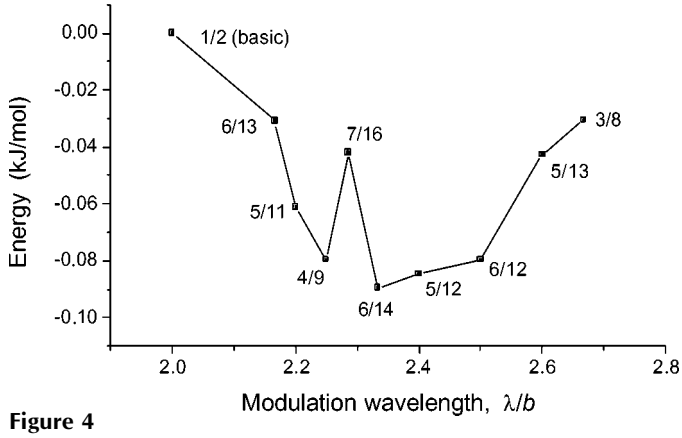

Figure 4
Lattice energies of the simulated superstructures of biphenyl plotted against the twist-angle modulation wavelength λ. The calculated points (squares) are marked with ratios $k = M/N$ (= b/λ), where M is the number of folds of the modulation wave per one N-fold supercell dimension, $bN = Nb$. The k = 1/2 case corresponds to the basic structure, with its energy taken as the zero reference point. Solid lines connecting the squares serve as a guide to the eye.

in the minimized structure (as illustrated in Fig. 3). The $k = 1/2$ case corresponds to the basic structure. The lowest energy was found with $k = 6/14$ (Table 6), which thus represents the global minimum of biphenyl with our model potential. The maximum amplitude of the twist angle is $\tau_{max} = 15^\circ$ in both the 6/13 and 6/14 structures (Fig. 3). The program *CRYCOM* revealed no extra symmetry in structure 6/14 over *Pa*, except for the presence of the pseudo-translation 0,1/2,0 as accurate as given by the r.m.s. deviations of 0.01 Å in the positions of the respective atoms, and 0.4° in the phenyl-ring rotations.

The energy levels in Fig. 4 differ by rather small quantities; nevertheless, they are significant with regard to the accuracy of their computation. As a matter of fact, the numerical accuracy in the energies of structures 6/13 and 6/14 caused by the distance truncation errors has been characterized by the test calculations of Table 3 to be within 0.0001 kJ mol^{-1}. Furthermore, it should be stressed that each modulated structure has been observed in the global minimization results many times (as the same or symmetry minima), having originated from different starting points. In such events, the minimal energy of a unique structure was reproduced with high accuracy. In particular, the energy scatter between the first- and the tenth-lowest energy values reached for the same structure (6/13 or 6/14) from different starting points was less than 0.002 kJ mol^{-1}.

3.5. Effect of pressure on the biphenyl structure

The availability of high-pressure experimental data on the biphenyl phases (Cailleau, 1986; Cailleau *et al.*, 1986; Moussa *et al.*, 1987) provides an extra opportunity to verify our model. To take the hydrostatic pressure into account, the enthalpy $H = E + PV$ was minimized (Dzyabchenko & Bazilevskii, 1985). Here E is the lattice energy, and V is the unit-cell volume per molecule. At normal pressure, the high-temperature state is represented by a stationary point of the energy hypersurface, 0.20 kJ mol^{-1} above the basic structure (Table 6) but, under minimal symmetry constraints such as $P2_1$, $Z = 2$, it can be treated at high pressure like a regular minimum. The basic and the modulated states 6/13 and 6/14 are more stable than the high-temperature structure (Table 6). At the same time, the former three have looser packings than the high-temperature structure, as follows from a comparison of their densities in Table 6. Consequently, one can expect that the imposition of pressure should stabilize the high-temperature form against the other states. Numerical calculations confirm this idea (Fig. 5). It can be seen that as the pressure increases form zero to 0.5 GPa, the curve for the high-temperature state approaches the curves for the other states. At still higher pressures, the four functions show a clear trend to merge with one another. On the other hand, the structures of the low-energy states exhibit a decrease in $\tau_{r.m.s.}$ with pressure down to nearly zero as the modulated superstructures transform into the ordinary high-temperature structure (Fig. 6). These results can be compared with the experimental P–T phase diagram of biphenyl (Cailleau, 1986; Cailleau *et al.*, 1986) showing the presence of only phase I above 0.17 GPa at zero temperature. Wasiutynski & Cailleau (1992) reproduced this diagram precisely by a lattice dynamical calculation of the phase transition I–II. Their model of the temperature-dependent intramolecular potential was calibrated on the points of the experimental diagram at 0 and 0.1 GPa. In contrast, our estimate of the critical pressure for the ground state of about 0.5 GPa is obtained *ab initio* and, in view of the very small differences in the slopes of the curves for the high-temperature and other states, it can be accepted as quite satisfactory.

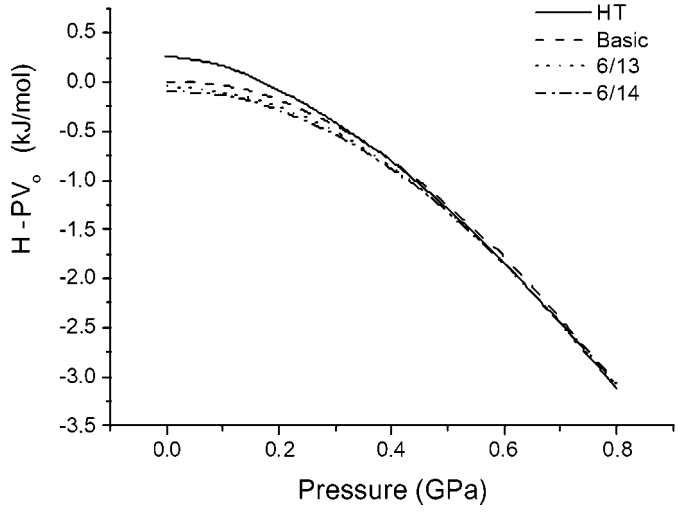

Figure 5
Plots of enthalpy minus PV_o/Z *versus* pressure. V_o is the cell volume of the basic structure at normal pressure.

4. Conclusions

Under minimal treatment of the molecular torsional potential energy (one adjustable parameter), we have elaborated a model of solid biphenyl that is generally consistent with experimental evidence on the structural changes and thermodynamic stability of the biphenyl phases in the phase transitions at low temperature. The model describes phase I of

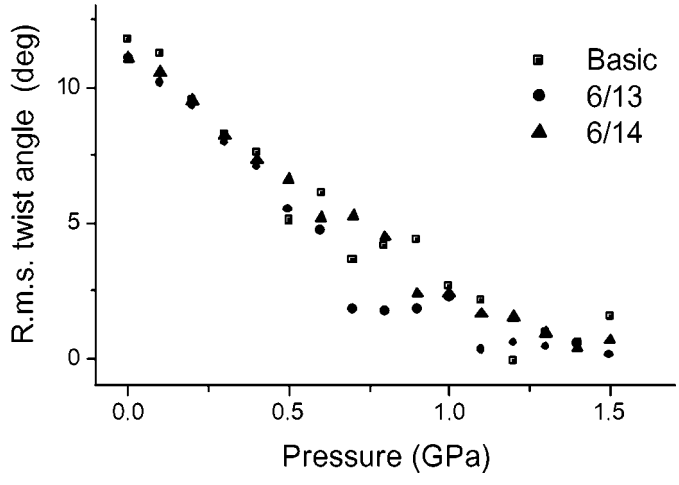

Figure 6
The effect of pressure on the r.m.s. twist angle.

the planar molecules as a stationary point of the energy function at the height ΔE separating the symmetry minima of the ground state III with the molecule twisted in the opposite sense; the low energy gap ΔE of 0.2 kJ mol^{-1} is consistent in order of magnitude with the experimentally observed transition temperatures. The global energy minimization reveals numerous low-energy structures of biphenyl that are basically similar; their common feature is the presence of dense molecular layers, which contain characteristic rows of molecules twisted cooperatively in the superstructure *b* direction. A number of structures of $P\bar{1}$ symmetry, with the twisted molecules in a general position, occur in the energy interval between the basic and the high-temperature structures. Their pseudomonoclinic lattice dimensions are approximate multiples of the dimensions of the basic structure, while the corresponding *b*-rows are generally different in the sign of the twist angle. One of these structures is similar to the low-temperature structure of quaterphenyl. Superstructure calculations show a reduction of the minimized energy for structures with twist-angle modulation, with the global minimum for structure k = 6/14 compared with the experimentally observed 6/13. Under pressure, the ground-state structure changes gradually to the high-temperature structure. The physical origin of the incommensurate phase modulation in the ground state of biphenyl is, therefore, energetic in nature. It can be understood as the result of an unusual competition between the intramolecular and the crystal packing forces, which is resolved in a high-order superstructure. The periodic modulation waves seem to result from the trend of the quasi-one-dimensional system towards regularity that minimizes its internal strains in a compromise with the crystal periodicity.

This work was supported by a grant from the National Science Foundation (MCB 00–03722).

References

Almenningen, A., Bastiansen, O., Fernholt, L., Cyvin, B. N., Cyvin, S. J. & Samdal, S. (1985). *J. Mol. Struct.* **128**, 59–76.

Baudour, J. L., Delugeard, Y. & Cailleau, H. (1976). *Acta Cryst.* B**32**, 150–154.

Baudour, J. L., Delugeard, Y. & Rivet, P. (1978). *Acta Cryst.* B**34**, 625–628.

Baudour, J. L. & Sanquer, M. (1983). *Acta Cryst.* B**39**, 75–84.

Baudour, J. L., Toupet, L., Delugeard, Y. & Ghémid, S. (1986). *Acta Cryst.* C**42**, 1211–1217.

Belsky, V. K., Zorkaya, O. N. & Zorky, P. M. (1995). *Acta Cryst.* A**51**, 473–481.

Benkert, C., Heine, V. & Simmons, E. H. (1987). *J. Phys. C*, **20**, 3337–3354.

Brock, C. P. (1979). *Mol. Cryst. Liq. Cryst.* **52**, 157–162.

Bree, A. & Edelson, M. (1978). *Chem. Phys. Lett.* **55**, 319–322.

Busing, W. R. (1983). *Acta Cryst.* A**39**, 340–347.

Cailleau, H. (1986). *Incommensurate Phases in Dielectrics*, edited by R. Blink & A. P. Levanyuk, Vol. 2, pp. 71–99. Amsterdam: North Holland.

Cailleau, H., Baudour, J. L. & Zeyen, C. M. E. (1979). *Acta Cryst.* B**35**, 426–432.

Cailleau, H., Messager, J. C., Moussa, F., Bugaut, F., Zeyen, C. M. E. & Vettier, C. (1986). *Ferroelectrics*, **87**, 3–14.

Casalone, G., Mariani, C., Mugnoli, A. & Simonetta, M. (1968). *Mol. Phys.* **15**, 339–348.

Charbonneau, G.-P. & Delugeard, Y. (1976). *Acta Cryst.* B**32**, 1420–1423.

Charbonneau, G. P. & Delugeard, Y. (1977). *Acta Cryst.* B**33**, 1586–1588.

Corish, J., Morton-Blake, D. A., O'Donoghue, F., Baudour, J. L., Bénière, F. & Toudic, B. (1995). *J. Mol. Struct. (Theochem.)* **358**, 29–38.

Delugeard, Y., Desuche, J. & Baudour, J. L (1976). *Acta Cryst.* B**32**, 702–705.

Dzyabchenko, A. V. (1983). *Acta Cryst.* A**39**, 941–946.

Dzyabchenko, A. V. (1984*a*). *J. Struct. Chem.* **25**, 416–420.

Dzyabchenko, A. V. (1984*b*). *J. Struct. Chem.* **25**, 559–563.

Dzyabchenko, A. V. (1987). *J. Struct. Chem.* **28**, 862–869.

Dzyabchenko, A. V. (1989). *Sov. Phys. Crystallogr.* **34**, 131–133.

Dzyabchenko, A. V. (1994). *Acta Cryst.* B**50**, 414–425.

Dzyabchenko, A. V. (2001). *PMC*, Version 2001. Karpov Institute of Physical Chemistry, Moscow.

Dzyabchenko, A. V. & Agafonov, V. (1995). In *Proc. of the 28th Hawaii Int. Conf. on System Sciences*, Vol. 5, *Biotechnology Computing*, edited by L. Hunter & B. D. Shriver, pp. 237–245. Los Alamitos, California, USA: IEEE Computing Society Press.

Dzyabchenko, A. V. & Bazilevskii, M. V. (1985). *J. Struct. Chem.* **26**, 558–564.

Dzyabchenko, A. V., Pivina, T. S. & Arnautova, E. A. (1996). *J. Mol. Struct.* **378**, 67–82.

Ecolivet, C., Sanquer, M., Pellegrin, J. & DeWitte, J. (1983). *J. Chem. Phys.* **78**, 6317–6324.

Eijck, B. P. van (2002). *J. Comput. Chem.* **23**, 456–462.

Eijck, B. P. van, Spek, A. L., Mooij, W. T. M. & Kroon, J. (1998). *Acta Cryst.* B**54**, 291–299.

Gibson, K. D. & Scheraga, H. A. (1995). *J. Phys. Chem.* **99**, 3765–3773.

Heine, V. & Price, S. L. (1985). *J. Phys. C*, **18**, 5259–5278.

Hirshfeld, F. L. (1968). *Acta Cryst.* A**24**, 301–311.

Ishibashi, Y. (1981). *J. Phys. Soc. Jpn*, **50**, 1255–1258.

Launois, P., Moussa, F., Lemée-Cailleau, M. H. & Cailleau, H. (1989). *Phys. Rev. B*, **40**, 5042–5055.

Moussa, F., Launois, P., Lemée, M. H. & Cailleau, H. (1987). *Phys. Rev. B*, **36**, 8951–8954.

Natkaniec, I., Bielushkin, A. V. & Wasiutynski, T. (1981). *Phys. Status Solidus B*, **105**, 413–423.

Parlinski, K., Schranz, W. & Kabelka, H. (1989). *Phys. Rev. B*, **39**, 488–494.

Plakida, N. M., Belushkin, A. V., Natkaniec, I. & Wasiutynski, T. (1983). *Phys. Status Solidus B*, **118**, 129–133.

Takeuchi, H., Suzuki, S., Dianoux, A. J. & Allen, G. (1981). *Chem. Phys.* **55**, 153–162.

Tsuzuki, S., Uchimaru, T., Matsumura, K., Mikami, M. & Tanabe, K. (1999). *J. Chem. Phys.* **110**, 2858–2861.

Wasiutynski, T. & Cailleau, H. (1992). *J. Phys. Condens. Matter*, **4**, 6241–6252.

Williams, D. E. (1971). *Acta Cryst.* A**27**, 452–455.

Williams, D. E. & Starr, T. L. (1977). *Comput. Chem.* **1**, 173–177.